Theoretical Limits on Multiuser Molecular Communication in Internet of Nano-Bio Things

Ergin Dinc, *Member, IEEE,* Ozgur B. Akan, *Fellow, IEEE*

***Abstract*—In nano-bio networks, multiple transmitter-receiver pairs will operate in the same medium. Both inter-symbol interference and multi-user interference can cause saturation at the receiver side, and this effect may cause an outage. Thus, we propose a tractable framework to calculate the theoretical operating points for fully absorbing receiver.**

***Index Terms*—Molecular Communications, Absorbing Receiver, Stochastic Geometry, Interference Modeling**

I. Introduction

MOLECULAR communication (MC) has attracted significant research attention by having very wide possible application areas such as bio-hybrid systems, nanoscale sensing, intelligent drug delivery and body area networks [1], [2]. [3] introduces Internet of Bio-Nano Things (IoBNT) concept, where MC can be utilized in applications such as intra-body sensing and actuation networks, and environmental control pollution. [4] presents the architecture of MC. In addition, the medical applications of MC in diagnosis and treatment are discussed in [5]. The possible body area nanonetworks applications of nanomachines are investigated in [6].

MC is paving way for IoBNT, where high number of molecular devices will operate in the same medium. In IoBNT, multiple transmitter-receiver pairs will operate in the same medium. The easiest solution to tackle the interference problem is utilizing different molecules for different transmitter-receiver pairs. We consider this case highly unlikely because there will be many nanomachines working at the same volume. Therefore, we assume that the transmitters will use same molecule to communicate. Both Inter-symbol Interference (ISI) and Multi-user Interference (MUI) will create significant limits in the communication network. For this reason, we investigate the effects of ISI and MUI for a realistic fully absorbing receiver model, where the receiver can only absorb number of molecules lower than a threshold.

Existing studies mostly focus on modeling ISI in the communication link for point-to-point links [7]. The closest work to this paper is presented in [9], [10]. First, [10] provides the statistical modeling of the multiuser interference by using spatial homogeneous Poisson process with the assumption of white Gaussian transmit signals. In addition, [9] proposes an analytical framework based on poisson point process (PPP) to model the collective signaling for passive receiver and fully absorbing receiver.

The contributions of this paper are two-fold. First, we propose an analytical framework for the expected number of molecules received at absorbing receiver volume by considering both ISI and MUI. [9] only considers the interference coming from other transmitters at the same signaling time. However, previous signals have a significant contribution in interference level as well. [10] only considers the interference statistics at the receiver, but we propose the exact expressions for ISI and MUI in this paper. The second main contribution of this work is investigating receiver operation points in terms of user density and the number of molecules that can be absorbed by the receiver at each observation time. We assume a more realistic receiver model in which the receiver saturates after a certain number of molecules. Therefore, this saturation effect causes an outage in MC link. The proposed theoretical framework is utilized to determine the maximum user density that can operate at the same time for the first time in the literature. At the end, the results of this study can be utilized in designing realistic MC networks.

The remainder of the paper is organized as follows. Section II includes the system model for the interference modeling. Theoretical modeling of ISI and MUI is proposed in Section III. Section IV provides the operating points for the receiver. The conclusions are presented in Section V.

II. System Model and Problem Definition

This section includes the MC channel and system model for interference modeling.

A. System Model

In this paper, we focus on the theoretical limitations on the number of active transmitters that can be present in a certain volume. This limitation results from the saturation in the receiver. Most of the literature assumes that the receiver can detect every molecule in the receive range. However, this assumption is highly unrealistic. In real world scenarios, receiver will have a certain number of receptor to detect the information carrying molecules. As in Fig. 1, we model the receiver as an absorbing receiver that can detect the molecules from a certain volume with radius (r_r) and saturates after a certain threshold (N_{RX}^{TH}) in the observation time interval (T_O).

Interference caused by ISI and MUI can limit the receiver performance. In Section III, we investigate both interference types and develop an analytical framework to calculate its

E. Dinc is with the Next-generation and Wireless Communications Laboratory, Department of Electrical and Electronics Engineering, Koc University, Istanbul, 34450 Turkey (e-mail: edinc@ku.edu.tr).

O. B. Akan is with the Internet of Everything Group, Electrical Engineering Division, Department of Engineering, University of Cambridge, UK, CB3 0FA, and the Next-generation and Wireless Communications Laboratory, Department of Electrical and Electronics Engineering, Koc University, Istanbul 34450, Turkey (e-mail: oba21@cam.ac.uk, akan@ku.edu.tr).

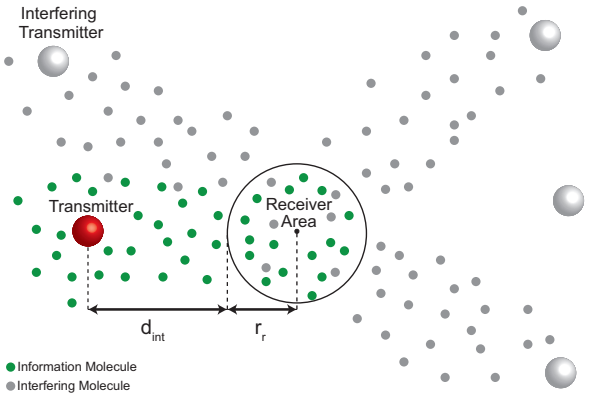

Fig. 1. System Model (Information molecules and interfering molecules are the same type.)

level without time consuming Monte-Carlo simulations. We investigate a spherical volume such as a drop of blood or a targeted tissue, where multiple nanomachines/nanosensors operate as a transmitter. Both receiver and transmitters are in the spherical volume with the radius of R_D. We assume that each transmitter has a target node to communicate, but we only investigate the interference in the intended receiver because the behavior of this single receiver can be generalized for other receiving nodes. In addition, there will be no interfering transmitter closer than than the active transmitter.

Locations of the interfering transmitters are determined randomly. The intended receiver has a transmitting node which is separated by a distance d_{int} from the receive range of the receiver. This paper do not consider the detection of the signals at the receiver. Instead, the operating points for the receiver in a large-scale IoBNT is investigated to provide the receiver not to have saturation due to ISI and MUI. If the receiver can observe the incoming signals without having saturation, the incoming information can be estimated by using the various techniques already proposed for MC ([4] provides good summary for MC.). We also assume that the receiver absorbs all the molecules at the end of the observation time and become ready to absorb hitting molecules in the next time span.

B. Molecular Communication Channel

The absorbing receiver is modeled as a 3D spherical volume as in Fig. 1. MC channel can be modeled with diffusion-based or flow-based models. In this study, we utilize the well-known diffusion based model [8]. In addition, the flow-based models are especially suitable to model diffusion, collisions, and flow effects, for example, in blood vessels [11].

[8] provides an analytical framework to model MC via diffusion with an absorbing receiver, and we also utilize this framework to model the channel. We use on-off keying based modulation, where transmitters release molecules only for bit 1, and molecule release is instant. The number of expected molecules hitting to the receiver Ω_r for fully absorbing receiver between $[t, t+\Delta t]$ can be found as [8]

$$\mathrm{E}(\Omega_r|d,t) = \frac{r_r}{d+r_r}\left[\mathrm{erfc}\left(d/\sqrt{4\pi D(t+\Delta t)}\right) - \mathrm{erfc}\left(d/\sqrt{4\pi D t}\right)\right], \quad (1)$$

where r_r is the radius of the receive range, d is the shortest distance between the point transmitter and the receive range (the distance between the transmitter and the center of the receiver is $d+r_r$ as in Fig. 1), D is the diffusion constant which depends on the temperature, viscosity and size of the molecule [12], $erfc(.)$ is the complementary error function.

Fig. 2 shows the number of molecules that are absorbed by the receiver. As noticed, the receiver absorbs 280 molecules in the peak time and the molecule count degrades as the time past. Fig. 3 shows the molecule absorbed at the receiver located at the center for random data stream. Fig. 3(a) shows the molecule transmission between intended transmitter and receiver. The molecule level increases as the time past due to ISI. For 20 interfering transmitters, MUI level can exceed 2000 molecule count as shown in Fig. 3(b). If the saturation point of the receiver is below the sum of ISI and MUI, the receiver will be saturated and assume every transmitted bit as 1. Therefore, the number of active transmitters in a certain volume cannot exceed a threshold that depends on receiver specifications. To this end, we propose a theoretical model to determine the safe operating points for multiuser MC.

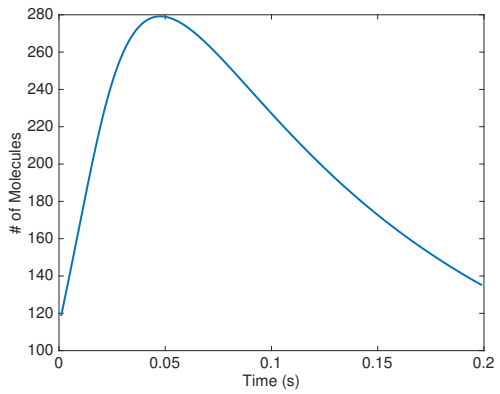

Fig. 2. Molecule count at the receiver for a single bit 1 for $d_{int} = 10\mu$m, $r_0 = 10\mu$m, $D = 79.4\mu\text{m}^2$, $M = 5000$ mol., and $T_O = 0.05$s.

III. Theoretical Modeling of ISI and MUI

In this section, we propose theoretical modeling of ISI and MUI. At the end, PPP based MUI model is developed.

A. ISI Model

ISI causes a significant increase in the molecule count level in the receiver volume as in Fig. 3(a). The expected ISI level can be calculated as the sum of all remaining molecules from previous symbols as

$$\mathrm{E}[N_{ISI}|N_D, d_{int}, T] = \mathrm{E}\left[M \sum_{n=1}^{N_D-1} b_n \mathrm{E}(\Omega_r, d_{int}, T - nT_S)\right], \quad (2)$$

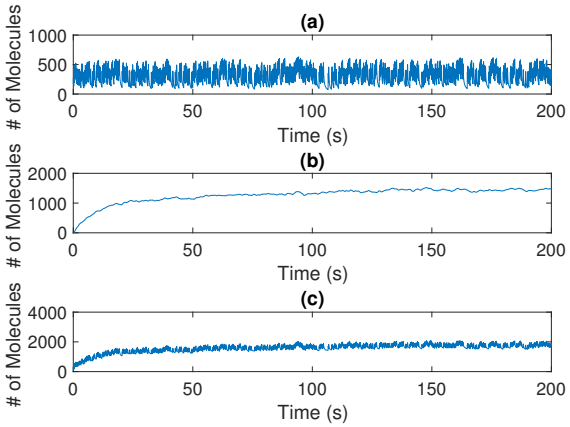

Fig. 3. Molecule count at the receiver vs. data length size for (a) intended transmitter to receiver, (b) interference from other transmitters, and (c) total number of molecules at the receiver volume for $R_D = 100\mu$m, $T_S = 0.2$s signaling time, $N_D = 1000$ data length and $N_I = 20$ number of interferers.

where M is the number of molecules released from the transmitter, T_S is the time interval between the signals, $b_n \in \{0, 1\}$ is the nth symbol, and N_D is the number of symbols. In (2), only randomness is on b_n that follows the Bernoulli distribution with equal probabilities. Thus, the expression is simplified as

$$\mathrm{E}[N_{ISI}|N_D, d_{int}, T] = M \sum_{n=1}^{N_D-1} \mathrm{E}(\Omega_r, d_{int}, T - nT_S)\mathrm{E}\left[b_n\right], \\ = \frac{M}{2} \sum_{n=1}^{N_D-1} \mathrm{E}(\Omega_r, d_{int}, T - nT_S). \quad (3)$$

Fig. 4 shows the theoretical and simulation results for SISO MC. As noticed, the level of the ISI increases and stabilizes after a certain time. The theoretical curve estimated with (3) is consistent with the simulation results. 290 molecules are absorbed by the receiver in the stable condition due to ISI. This result can be utilized for adaptive detection studies.

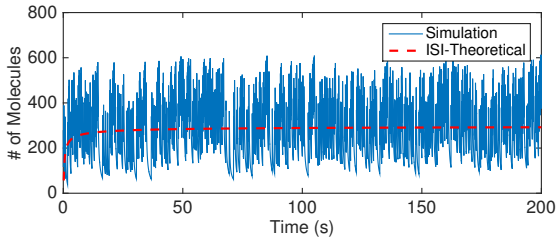

Fig. 4. ISI at the receiver volume for $R_D = 100\mu$m, $d_{int} = 10\mu$m, $r_r = 10\mu$m, $D = 79.4\mu$m^2, $M = 5000$ mol., $N_D = 1000$ $T_O = 0.05$s and $T_S = 0.2$.

B. MUI Model

MUI results from the molecule release by interfering transmitters. Both current and previous molecule releases will create interference at the receiver volume. For this reason, theoretical estimations are required to consider ISI coming from the interfering nodes as well. To this end, MUI at the receiver is estimated as

$$\mathrm{E}[N_{MUI}|N_D, N_I, \mathbf{d}, T] = \frac{M}{2} \sum_{i=1}^{N_I} \sum_{n=1}^{N_D} \mathrm{E}(\Omega_r, r_i, T - nT_S), \quad (4)$$

where $\mathbf{d}$ is a vector containing the distance between the transmitter and the closest point to the receiver volume. The theoretical MUI estimation only requires the distance vector. In this calculation, we assume that all the transmitters are synchronized and release the molecules at the same time. Since the behavior of the unsynchronized case is almost the same with the synchronized one, we use the synchronized transmitters assumption for simplicity.

Fig. 5 shows the simulation results and theoretical estimations of MUI. The theoretical and simulation results are consistent with each other. The simulation results fluctuate around the theoretical curve due to the random locations of the interfering transmitters. This deviation from the theoretical MUI curve is close to the Gaussian distribution as presented in Fig. 6.

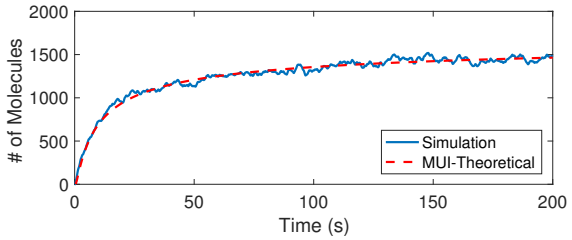

Fig. 5. MUI at the receiver volume for $R_D = 100\mu$m, $d_{int} = 10\mu$m, $r_r = 10\mu$m, $D = 79.4\mu$m^2, $M = 5000$ mol., $N_D = 1000$, $N_I = 20$, $T_O = 0.05$s and $T_S = 0.2$.

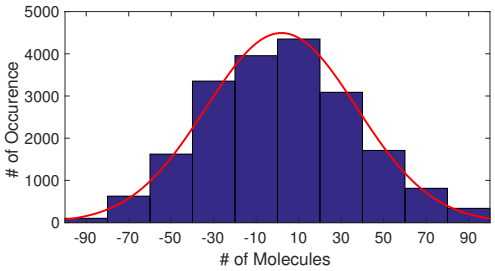

Fig. 6. Histogram of deviations from the theoretical MUI model with Gaussian distribution fitting ($\mathcal{N}(1.9, 35.5)$).

C. PPP based MUI Model

Stochastic geometry is a powerful method to avoid the randomness coming from the locations of the transmitters, and it is highly utilized in telecommunication to model the random spatial distribution of the users in cellular networks [13]. In [9], 3D-stochastic geometry based on PPP is utilized to model the interference coming from interfering molecular transmitters. However, this work does not include the previous symbols coming from the interfering stations. We also utilize

PPP to investigate the level of MUI in a certain volume where the transmitter and receiver can take random positions.

In PPP, the nearest neighbor function gives the probability of having a node closer than R, and defined for 3D as

$$\mathrm{P}(r \leq R) = F_r(R) = 1 - e^{\left(-\lambda \frac{4}{3}\pi r^3\right)}, \tag{5}$$

where $\lambda = 2/(4/3\pi R_D^3)$ is the node density in the volume for a transmitter and receiver. Therefore, the probability density function (PDF) can be defined as

$$f_r(r) = 4\lambda\pi r^2 e^{\left(-\lambda \frac{4}{3}\pi r^3\right)}. \tag{6}$$

By using PPP, we can remove the randomness in (5), and the expression is simplified as

$$\begin{aligned}
\mathrm{E}[N_{MUI}|N_D, N_I, T] &= \int_{r_r}^{\infty} \mathrm{E}[N_{MUI}|N_D, N_I, r, T] f_r(r) dr, \\
&= \int_{r_r}^{\infty} \frac{M}{2} \sum_{i=1}^{N_I} \sum_{n=1}^{N_D} \mathrm{E}(\Omega_r, r, T - nT_S) 4\lambda\pi r^2 e^{\left(-\lambda \frac{4}{3}\pi r^3\right)} dr, \\
&= \frac{M}{2} \sum_{i=1}^{N_I} \sum_{n=1}^{N_D} \int_{r_r}^{\infty} \mathrm{E}(\Omega_r, r, T - nT_S) 4\lambda\pi r^2 e^{\left(-\lambda \frac{4}{3}\pi r^3\right)} dr.
\end{aligned} \tag{7}$$

The boundary of the integral starts from r_r because the transmitter cannot be placed inside the receiver volume. As noticed from (7), the index i has no effect in the integral. Therefore, the expected MUI can be simplified as

$$\begin{aligned}
\mathrm{E}[N_{MUI}|N_D, N_I, T] = \frac{N_I M}{2} \sum_{n=1}^{N_D} \int_{r_r}^{\infty} \mathrm{E}(\Omega_r, r, T - nT_S) \\
\times 4\lambda\pi r^2 e^{\left(-\lambda \frac{4}{3}\pi r^3\right)} dr.
\end{aligned} \tag{8}$$

Fig. 7 shows the simulation and theoretical results for the number of MUI molecules vs. the number of interfering transmitters for $N_D = 1000$. The simulation results presented in Fig. 7 is the average case results. The relationship between MUI and the number of interfering transmitters is linear and the theoretical model is very close to the simulation results. The actual distribution of the MUI simulation results for 1 interfering transmitter are presented in Fig. 8. As noticed, the actual distribution of MUI can be fitted with an exponential distribution with mean $\mathrm{E}[N_{MUI}|N_D, N_I, T] = 70.6$ ($\mathcal{E}(\mathrm{E}[N_{MUI}|N_D, N_I, T])$). Therefore, MUI for N_I number of interferers can be estimated with the sum of exponential distributions, and can be modeled as the Gamma distribution with the shape factor of N_I and the scale factor of $\mathrm{E}[N_{MUI}|N_D, N_I, T]$ as ($\mathcal{G}(N_I, \mathrm{E}[N_{MUI}|N_D, N_I, T])$).

IV. Theoretical Limits on Multiuser Molecular Communication

In the previous sections, a tractable framework is proposed to calculate both ISI and MUI effects. In this section, we use this framework to calculate the maximum number of transmitters that can operate in a spherical volume. If the interference is higher than the number of molecules that can be absorbed by the receiver, the receiver will saturate and the

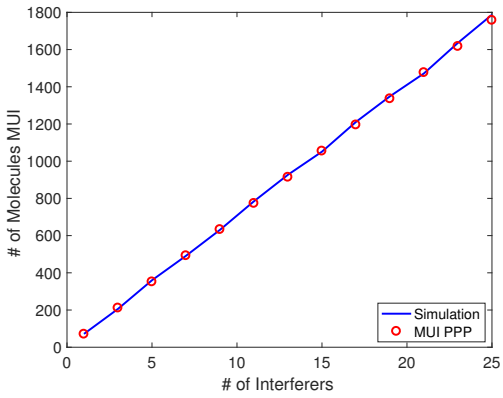

Fig. 7. MUI vs. the number of interfering transmitters with simulation results and theoretical calculations with PPP.

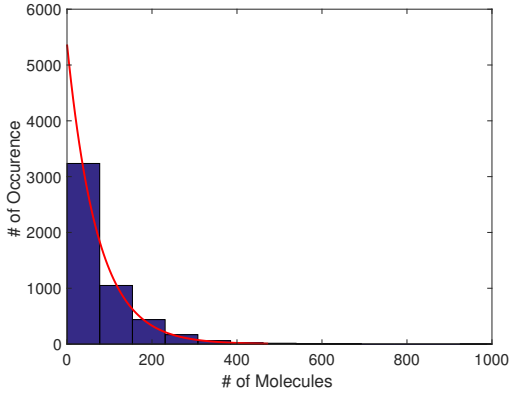

Fig. 8. Histogram of the MUI simulation results for 1 interfering transmitter with exponential fitting ($\mathcal{E}(\mathrm{E}[N_{MUI}|N_D, N_I, T] = 70.6)$).

communication link will have an outage. The total amount of expected interference can be estimated with

$$\begin{aligned}
N_{Total}^I = \mathrm{E}[N_{ISI}|N_D, d_{int}, T] + \\
\mathcal{G}(N_I, \mathrm{E}[N_{MUI}|N_D, N_I, T]) + \mathcal{N}(\mu_{MUI}, \sigma_{MUI}),
\end{aligned} \tag{9}$$

where μ_{MUI} and σ_{MUI} is the mean and standard deviation for the deviations from the theoretical MUI model as presented in Fig. 6. In (10), N_M^{SISO} and $\mathrm{E}[N_{ISI}|N_D, d_{int}, T]$ can be directly calculated by just knowing the distance between intended transmitter and receiver. For the observation time, we choose the time associated with the $N_D = 1000^{\text{th}}$ symbol ($T = N_D T_S$) in which the level of both ISI and MUI stabilizes. After 1000 iterations, we found the average values for $\mu_{MUI} = 0.24$ and $\sigma_{MUI} = 54.6$.

In Fig. 2, a single signal without any interference is presented for $d_{int} = 10\mu$m. The molecule count reaches $N_M^{SISO} = 280$ at the maximum case. To observe the full signal in the multi-user case, the receiver requires to have an absorption threshold such that

$$N_{RX}^{TH} \geq N_M^{SISO} + N_{Total}^I. \tag{10}$$

Fig. 9 shows the operating points for observing the full wave at the absorbing receiver for 0.99 non-exceeding percentage. That is, the receiver can operate without having any saturation

due to ISI and MUI for the 99% of the time. As noticed, the relationship between the maximum number of interferers and molecule threshold is almost linear.

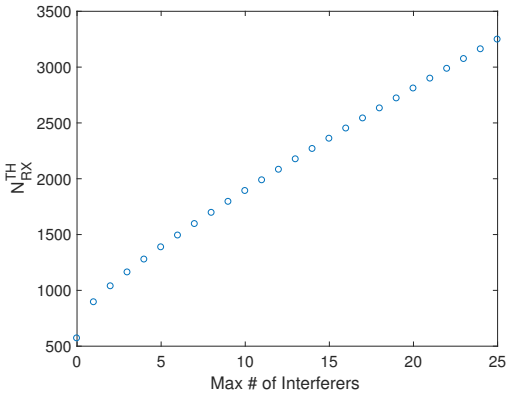

Fig. 9. Receiver operating points for $R_D = 100\mu$m, $d_{int} = 10\mu$m, $r_r = 10\mu$m, $D = 79.4\mu\text{m}^2$, $M = 5000$ mol., $N_D = 1000$, $T_O = 0.05$s and $T_S = 0.2$.

V. Conclusion and Future Work

In this paper, we propose a tractable framework to calculate ISI and MUI in MC networks. Most importantly, the safe operating points for the receiver threshold and the number of active transmitters are presented. The results of this paper can be utilized to develop adaptive MC modulation and operating points for nano-networks.

ACKNOWLEDGEMENT

This work was supported in part by the ERC project MINERVA (ERC-2013-CoG #616922), and the EU project CIRCLE (EU-H2020-FET-Open #665564).

References

[1] O. B. Akan, *et al.*, "Fundamentals of Molecular Information and Communication Science," to appear in *Proc. IEEE*, 2016.

[2] B. Atakan, S. Galmes and O. B. Akan, "Nanoscale Communication With Molecular Arrays in Nanonetworks," *IEEE Trans. Nanobiosci.*, vol. 11, no. 2, pp. 149-160, June 2012.

[3] I. F. Akyildiz, M. Pierobon, S. Balasubramaniam and Y. Koucheryavy, "The internet of Bio-Nano things," *IEEE Communications Magazine*, vol. 53, no. 3, pp. 32-40, Mar. 2015.

[4] T. Nakano, *et al.*, "Molecular Communication Among Biological Nanomachines: A Layered Architecture and Research Issues," *IEEE Trans. Nanobiosci.*, vol. 13, no. 3, pp. 169-197, Sept. 2014.

[5] L. Felicetti, M. Femminella, G. Reali, P. Lio, "Applications of molecular communications to medicine: A survey," *Nano Communication Networks*, vol. 7, pp. 27-45, Mar. 2016.

[6] B. Atakan, O. B. Akan and S. Balasubramaniam, "Body area nanonetworks with molecular communications in nanomedicine," *IEEE Communications Magazine*, vol. 50, no. 1, pp. 28-34, Jan. 2012.

[7] A. Noel, K. C. Cheung, and R. Schober, "A unifying model for external noise sources and isi in diffusive molecular communication," *IEEE J. Sel. Areas Commun.*, vol. 32, no. 12, pp. 2330-2343, Dec 2014.

[8] H. B. Yilmaz, *et al.*, "Three-Dimensional Channel Characteristics for Molecular Communications With an Absorbing Receiver," *IEEE Commun. Lett.*, vol. 18, no. 6, pp. 929-932, June 2014.

[9] Y. Deng, *et al.*, "Stochastic Geometry Model for Large-Scale Molecular Communication Systems", in *Proc. IEEE GLOBECOM*, Dec. 2016.

[10] M. Pierobon, I. F. Akyildiz, "A Statistical-Physical Model of Interference in Diffusion-Based Molecular Nanonetworks," *IEEE Trans. Commun.*, vol. 62, no. 6, pp. 2085-2095, June 2014.

[11] L. Felicetti, M. Femminella, G. Reali, P. Gresele, M. Malvestiti, J. N. Daigle, "Modeling CD40-Based Molecular Communications in Blood Vessels," *IEEE Trans. Nanobiosci.*, vol. 13, no. 3, pp. 230-243, Sept. 2014.

[12] H. J. V. Tyrrell and K. Harris, Diffusion in liquids, A theoretical and experimental study. Butterworth Publishers, Stoneham, MA, 1984.

[13] J. G. Andrews, F. Baccelli and R. K. Ganti, "A Tractable Approach to Coverage and Rate in Cellular Networks," *IEEE Trans. Commun.*, vol. 59, no. 11, pp. 3122-3134, Nov. 2011.

Ergin Dinc [S'12, M'16] (edinc@ku.edu.tr) received his Ph.D. degree in Electrical and Electronics Engineering fromKoc University, Istanbul, Turkey in June 2016 under the supervision of Prof. Dr. Ozgur Baris Akan. He is currently a postdocat the School of Information and Communication Technology (ICT) of the Royal Institute of Technology (KTH) in Sweden. His current research interests include wireless, direct air-to-ground, beyond line-of-sight and molecular communications.

Ozgur B. Akan [M'00-SM'07-F'16] (oba21@cam.ac.uk) received his Ph.D. degree in electrical and computer engineering from the Broadband and Wireless Networking Laboratory, School of Electrical and Computer Engineering, Georgia Institute of Technology, Atlanta, GA, USA, in 2004. He is currently with the Electrical Engineering Division, Department of Engineering, University of Cambridge, UK. His research interests include wireless, nano, molecular communications, and Internet of everything.